

High-quality transparent conductive indium oxide films prepared by thermal evaporation

C. A. Pan and T. P. Ma

Yale University, Department of Engineering and Applied Science, New Haven, Connecticut 06520

(Received 17 March 1980; accepted for publication 7 May 1980)

Highly transparent (over 90% transmission in the visible range) and highly conductive (resistivity $\approx 2 \times 10^{-4} \Omega \text{ cm}$) indium oxide (undoped) films have been produced by thermal evaporation from an $\text{In} + \text{In}_2\text{O}_3$ source in a vacuum chamber containing low pressures of O_2 . These properties are comparable or superior to the best tin-doped indium oxide films ever reported, and excellent reproducibility has been achieved. Hall effect measurements have revealed that the observed low resistivity is primarily a result of the excellent electron mobility ($\approx 70 \text{ cm}^2/\text{V sec}$), although the electron concentration is also rather high ($> 4 \times 10^{20}/\text{cm}^3$). X-ray diffraction measurements show distinctly polycrystalline In_2O_3 structure with a lattice constant ranging from 10.07 to 10.11 Å. Electrolytic electroreflectance spectra exhibit at least four critical transitions, from which we have determined the direct and indirect optical band gaps (≈ 3.56 and 2.69 eV , respectively). Burstein shifts due to the population of electrons in the conduction band are also observed. These and other results along with a discussion of the processing details are reported.

PACS numbers: 81.15.Ef, 78.65.Jd, 73.60.Fw, 85.60. — q

Optically transparent electrically conducting films based on undoped or tin-doped indium oxide are useful in a variety of applications. The most commonly used preparation techniques include sputtering¹⁻⁶ and chemical spray deposition,⁷⁻⁹ but very little work has been done with thermal evaporation. In this letter, we report some remarkable electrical and optical properties of undoped indium oxide films prepared by a simple thermal evaporation technique. Films with low resistivity ($\approx 2 \times 10^{-4} \Omega \text{ cm}$) and high visible transmission (over 90%) have been readily obtained without postdeposition annealing. Although no tin dopant is used, these properties are comparable or superior to the best indium tin oxide (ITO) films ever reported, and excellent reproducibility has been achieved. Compared to the other techniques, the present technique is much simpler, and is easily accessible to anyone equipped with a vacuum evaporator.

The evaporation is done in a diffusion-pumped vacuum system with a resistance-heated source. The evaporation boat consists of an alumina crucible heated by a tungsten heater. A mixture of In_2O_3 powder and metallic In (approximately 90% In_2O_3 + 10% In by weight) is used as the source material. It has been found that the incorporation of the metallic In in the evaporation source not only significantly enhances the evaporation rate, but also dramatically improves the optical and the electrical properties of the films. Initially, the vacuum chamber is evacuated to a base pressure of approximately 1×10^{-6} Torr. Pure O_2 is then admitted to the chamber. With the high-vacuum valve remaining open, a steady-state chamber pressure ranging from 6×10^{-5} to 2×10^{-4} Torr is rapidly reached by adjusting the O_2 needle valve. A microscope cover glass (Scientific product) is used as the substrate, and a substrate heater maintains a temperature range from 320 to 350 °C. The evaporation rate is typically maintained in a range from 15 to 30 Å/min. The sheet resistance of the film is also monitored continuously during evaporation.

Figure 1 shows the sheet resistance as a function of film thickness. It can be seen that a sheet resistance of $6.75 \Omega/\square$ is reached at a film thickness of 2700 Å, corresponding to an average resistivity of $1.8 \times 10^{-4} \Omega \text{ cm}$. This value is comparable or superior to the typical values recently reported for sputtered ITO films,³⁻⁶ and is certainly far better than any In_2O_3 films ever reported. The film thickness is measured by an optical interference technique after which, when compared with the thickness data from the crystal monitor, results in an effective sticking probability of 0.6. The calculated differential sheet conductance per unit thickness $\Delta G/\Delta t$ is also shown in Fig. 1. It can be seen that the conductivity starts to rise very rapidly at about 50 Å. Whether this is due to the onset of a continuous film, or to the transition from a surface scattering-limited conduction to a bulk conduction process is not yet clear. The differential conductance, however, stays high beyond this transition region, as long as the

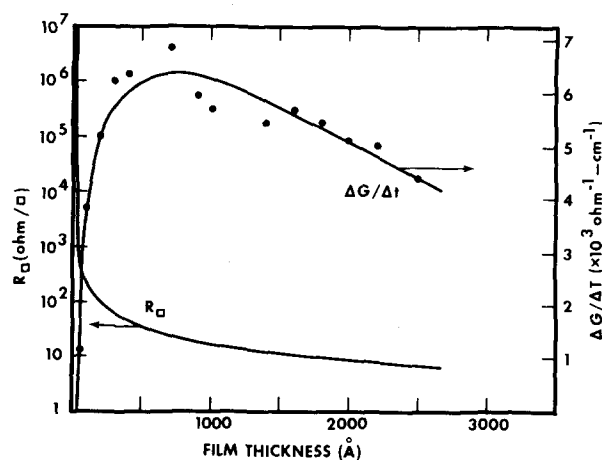


FIG. 1. Sheet resistance R_{\square} and sheet conductance per unit film thickness $\Delta G/\Delta t$ as a function of the In_2O_3 thickness.

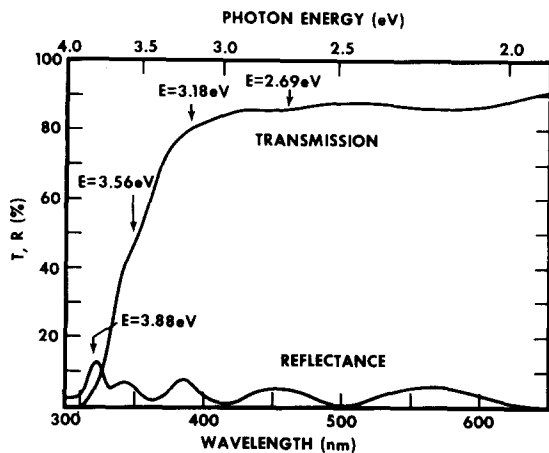


FIG. 2. Transmission (normal incidence) and reflectance (6° incident angle) of the thermally evaporated In_2O_3 film. Four optical critical points, as obtained by the electroreflectance spectra (see Fig. 3), are marked. Film thickness is 2700 \AA .

same experimental conditions are maintained.

Hall effect measurements have been made to determine the type of the conduction carriers, and their mobility and concentration. The room-temperature measurement results in a Hall mobility of $74 \text{ cm}^2/\text{V sec}$, and a free-electron concentration of $4.69 \times 10^{20} \text{ cm}^{-3}$. Such a high electron mobility has rarely been reported in In_2O_3 films, doped or undoped, and is largely responsible for the low resistivity in our samples. This improved electron mobility may be attributed to the lack of impurity scattering centers. At liquid-nitrogen temperature, the resistivity decreases slightly ($\approx 14\%$), while at 340°C in a vacuum environment, the resistivity increases ($\approx 66\%$). This suggests that the film is degenerate, and the metal-like temperature dependence primarily comes from the changes in mobility.

Figure 2 shows the optical transmission and the reflectivity of the film in the wavelength range from 300 to 600 nm. The transmission measurement is done in a normal incident mode, and the reflectivity is measured at an incident angle of 6° with respect to the normal vector. Using a silicon photodetector, the integrated transmission is measured to be 91%.

To determine the optical band gap of the film, we performed an electrolytic electroreflectance measurement, where the relative differential reflectance $\Delta R/R$, modulated by an applied ac field, is plotted as a function of optical wavelength. It has been well established that such spectra provide information about the optical critical points, and the principles of this technique can be found in several review articles.^{10,11} The sample configuration in the present experiment is similar to those reported by Williams¹² and by Shaklee *et al.*,¹³ where an aqueous solution of KCl served as our electrolyte, and a 40-Hz ac modulation (1.4V peak to peak) superimposed on a dc voltage (0.7 V) is applied between a platinum electrode and the indium oxide film. The reflected monochromatic light is detected by a photomultiplier, which generates an intensity-proportional voltage at its output. This voltage is manipulated by an electronic circuit, consisting of a lock-in amplifier and several operational amplifiers, to provide the ratio between the modulated reflectance

ΔR and the dc reflectance R .

Figure 3 shows the spectral dependence of the electroreflectance for the same sample under discussion. Following an analytical method developed by Aspnes,¹¹ we arrive at four critical energies, 3.88, 3.56, 3.18, and 2.69 eV. The second and the sharpest peak, centered around 3.56 eV, seems to be in good agreement with the direct-band-gap values (3.55–3.65 eV) previously obtained elsewhere by absorption measurements.^{15,16} The first peak, at 3.88 eV for this sample, has been found to depend on the free-electron concentration and is attributable to the Burstein shift¹⁷ of the direct absorption edge. Assuming a density-of-state effective mass of $0.55m_0$,^{9,16} the calculated Burstein shift due to the conduction-band electrons for this film (electron density = $4.69 \times 10^{20} \text{ cm}^{-3}$) is 0.4 eV, which compares closely with the difference between the above two critical points. The fourth critical point, at approximately 2.69 eV, agrees well with the reported indirect-band-gap transition¹ for In_2O_3 . The remaining critical point at approximately 3.18 eV may therefore be attributed to the Burstein shift of the indirect absorption edge. The amount of this shift, 0.49 eV, is larger than that associated with the direct absorption edge mentioned previously, and is due primarily to the smaller density-of-state effective mass associated with the indirect transition, although phonons may also play a role.

The fact that both the transition to the bottom of the conduction band and the transition to the Fermi level are observed in the same sample is remarkable. We believe this is a direct consequence of the electric field modulation of the depletion layer in the electroreflectance measurement. In the depletion layer, the conduction band is empty, and the transition is made to the bottom of the conduction band. At the edge of the depletion layer and in the bulk of the In_2O_3 film, the conduction band is filled to the Fermi level, and a Burstein shift is observed in the optical transition. The applied ac field modulates both the field strength and the width of the depletion layer, which in turn causes a change in the reflectance for both processes. A fuller account of our electroreflectance experiments will be reported elsewhere.

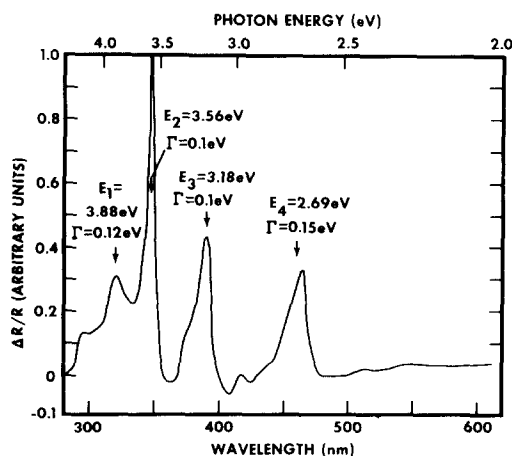


FIG. 3. Electroreflectance of the In_2O_3 film as a function of wavelength. Four critical energy points are marked, along with their broadening parameters Γ .

The x-ray diffraction data suggest that the film structure is primarily polycrystalline In_2O_3 . The values of the cubic lattice constant measurements for the films range from 10.07 to 10.11 Å, which are in good agreement with those reported by Wyckoff¹⁴ for bulk In_2O_3 (10.118 Å). The slightly smaller lattice constants that we observe may be related to the oxygen vacancies in our samples, which are also believed to be the source of conduction electrons.

Although in this letter we only report the results of one particular sample, we have achieved excellent reproducibility in our laboratory, with typical values of the film resistivity within 20% and the optical transmission within 5% of those reported here. The more significant processing parameters have been identified, and we found that several of these parameters must be controlled within a rather narrow range to produce optimum films. The empirically determined ranges are 15–30 Å/min for evaporation rate, 320–350 °C for substrate temperature, 5×10^{-5} – 2×10^{-4} Torr for oxygen partial pressure, and 5–20% for metallic In concentration in the source. Significant departure from these values seems always to result in less conductive films, although sometimes a reduced optical transmission is also observed. Another important effect which should not be overlooked is the possible chemical reaction between the indium oxide vapor and the Ta or W heater. This could occur if the heater element is in the flight path of the indium oxide vapor, and could result in an order-of-magnitude degradation of the conductivity. To avoid this, we recommend the use of a proper combination of crucible and heater element, such that the crucible is taller than the top edge of the heater. With such precaution taken, we have found no difficulty in reproducing the films within the range reported.

In summary, highly transparent and conductive indium

oxide films have been produced by a simple thermal evaporation technique. Although undoped, the conductivity and optical transmission of these films are comparable or superior to the best ITO films reported in the literature. The significant processing parameters that affect the film properties have been identified. A more systematic study of the processing parameters is in progress along with more elaborate measurements of the film properties. It would be interesting to determine the role that the metallic In plays in the evaporation kinetics and its contribution to film properties. Photovoltaic devices incorporating such films are also being investigated.

The authors gratefully acknowledge the support of this work by the National Science Foundation under Grants No. ECS-7906933 and ENG-7910888.

¹R. L. Weiher and R. P. Ley, J. Appl. Phys. 37, 299 (1966).

²H. K. Muller, Phys. Status Solidi 27, 723 (1968).

³D. B. Fraser and H. D. Cook, J. Electrochem. Soc. 119, 1368 (1972).

⁴W. W. Molzen, J. Vac. Sci. Technol. 12, 99 (1975).

⁵J. C. C. Fan, F. J. Bachner, and G. H. Foley, Appl. Phys. Lett. 31, 773 (1977).

⁶W. G. Haines and R. H. Bube, J. Appl. Phys. 49, 304 (1978).

⁷R. Groth, Phys. Status Solidi 14, 69 (1966).

⁸R. Claret, Appl. Phys. 2, 247 (1973).

⁹H. Kostlin, R. Jost, and W. Lems, Phys. Status Solidi (a) 29, 87 (1975).

¹⁰M. Cardona, *Modulation Spectroscopy* (Academic, New York, 1969).

¹¹D. E. Aspnes, Surf. Sci. 37, 418 (1973).

¹²R. Williams, Phys. Rev. 117, 1487 (1960).

¹³K. L. Shaklee, F. H. Pollak, and M. Cardona, Phys. Rev. Lett. 15, 883 (1965).

¹⁴R. W. G. Wyckoff, *Crystal Structures*, 2nd ed. (Wiley, New York, 1964), Vol. 2, p. 5.

¹⁵G. Rupprecht, Z. Phys. 139, 504 (1954).

¹⁶V. M. Vainshtein and V. I. Fistul, Sov. Phys. Semicond. 1, 104 (1967).

¹⁷E. Burstein, Phys. Rev. 93, 632 (1954).

Dependence of the electrical characteristics of heavily Ge-doped GaAs on molecular beam epitaxy growth parameters

G. M. Metze, R. A. Stall, C. E. C. Wood, and L. F. Eastman

School of Electrical Engineering and National Research and Resource Facility for Submicron Structures, Cornell University, Ithaca, New York 14853

(Received 8 February 1980; accepted for publication 6 May 1980)

Ge incorporation into molecular beam epitaxial GaAs as a function of substrate temperature (350–620 °C), Ge flux (10^9 – 10^{14} cm⁻² sec⁻¹) and of As₄/Ga flux ratio (10/1) has been studied. The free-electron (7.4×10^{19} cm⁻³) and free-hole (3.0×10^{20} cm⁻³) concentrations in GaAs were the highest obtained to date. Tentative incorporation mechanisms for Ge in GaAs are also presented.

PACS numbers: 73.60. – n, 68.55. + b, 81.15.Ef

Depending upon the growth conditions, either *n*- or *p*-type GaAs doped with Ge can be prepared.^{1,2} The ability to control both the free-carrier concentration and type, using a single dopant source, would be beneficial to molecular beam epitaxy (MBE), where effusion cell space is at a premium. Other properties of Ge, such as the ability to make abrupt

doping level changes, makes its use as a dopant in MBE very attractive.

To date, most MBE work has been primarily concerned with Ge concentrations N_{Ge} of 10^{16} – 10^{18} cm⁻³. However, it would be advantageous for nonalloyed ohmic contacts, tunnel diodes, etc., to be able to produce highly doped ($> 10^{19}$